The DC06 Outer Tracker Simulation

July 16, 2008

Abstract

This note gives an overview of the Outer Tracker simulation for the 2006 Data Challenge (DC06). It covers the Outer Tracker detector description used in Gauss/Geant to simulate hits in the Outer Tracker and the digitisation of the hits in Boole. It concludes with the expected performance of the Outer Tracker.

LHCb Note

Issue	Final
Revision	1
Reference	LHCb-2007-018
Created	July 16, 2008
Last Modified	July 16, 2008

Prepared by Jan Amoraal
NIKHEF, Amsterdam, The Netherlands

Jacopo Nardulli
NIKHEF, Amsterdam, The Netherlands

Contents

List of Tables

List of Figures

1 Introduction

The Outer Tracker (OT) [1] is a tracking detector based on straw tube technology. The OT together with the Inner Tracker (IT) [2], which is based on silicon strip technology, make up the tracking (T) stations T1, T2 and T3 located between the LHCb dipole magnet and RICH2. The information from the OT and the IT is used in the track reconstruction: the momenta of charged particles are determined from the reconstructed track segments in the T stations when combined with those in the Vertex Locater (VeLo) and in the Trigger Tracker (TT) (for more details on the tracking strategy and its performance see [3]).

This note gives an overview of the OT detector description, OT software and simulation, and concludes with the expected performance of the OT. The major changes with respect to DC04 are

- Realistic OT material budget and description.
- Realistic single cell efficiency based on 2005 test beam data.
- Increased the readout window from 50 ns to 75 ns.
- Gone from 24 Tell1s with 18 gols each to 48 Tells with 9 gols each

Other notes that might be of interest to the reader and that gives a detailed overview, albeit some are obsolete, of the development of the OT event model are [4, 5, 6, 7].

2 The Outer Tracker Detector Description

A new detector hierarchy was introduced for DC06 to speed-up the transport service and, ultimately, the track reconstruction and fitting. In the DC06 description the LHCb detector is split up into five regions: upstream, before magnet, magnet, after magnet and downstream, see Fig. 2.1. The tracking stations (comprised of the IT and OT) and the RICH2 are located in the after magnet region. This section covers the detector description of the OT.

The OT consists of three stations T1, T2 and T3. Each station is tilted in the LHCb frame[1] by an angle of 3.601 mrad and consists of four layers in the following stereo angle configuration $x(0°)$, $u(-5°)$, $v(5°)$ and $x(0°)$, as explained in [10]. The OT hierarchy is shown in Fig. 2.2. The combined setup of 2 vertical x layers with a u and v layers allow for efficient pattern recognition and provide precise coordinate measurements in the bending plane (x -

[1]For more details on the LHCb reference frame see Ref [8] and [9].

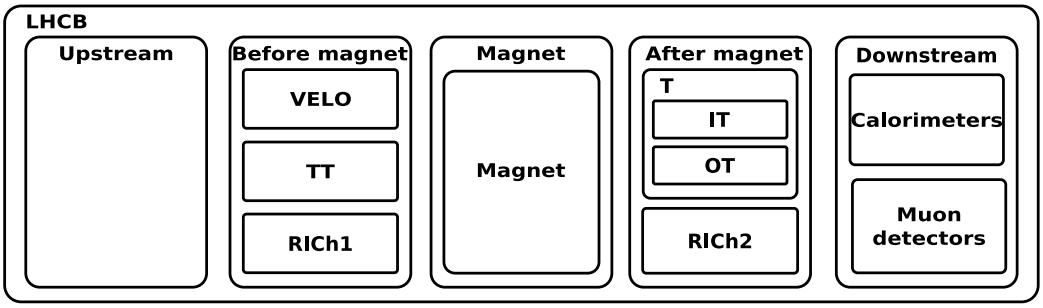

Fig. 2.1: DC06 LHCb detector hierarchy.

z_{cen} [mm]				
Station	X1	U	V	X2
T1 (7948)	7860.5	7915.5	7980.5	8035.5
T2 (8630)	8542.5	8597.5	8662.5	8717.5
T3 (9315)	9227.5	9282.5	9347.5	9402.5

Tab. 2.1: Z coordinates of the OT stations and layers.

z) and less, but sufficiently, precise measurements in the non-bending plane (y - z). Tab. 2.1 lists the z coordinates of the stations and layers.

Each layer consists of 22 modules: seven F (Full) modules to the left and seven F modules to the right of the beam pipe, and eight short (S1, S2 and S3) modules located around the beam pipe. Two layers, one x layer and one stereo layer, of modules are mounted onto a C-frame, 2 per station, which houses the electronics, cables and services. In the detector description the layers are divided into quarters to distinguish the read-out channels[2]. This also allows one to assign a unique "location" to a hit, which together with the TDC time of the hit, makes up the **OTChannelID**.

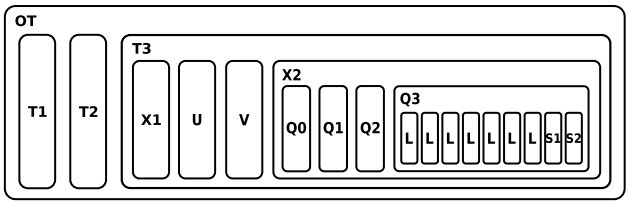

Fig. 2.2: OT hierarchy. Note only T3 is worked out, but T1 and T2 are similar.

Fig. 2.3(left) shows the configuration of the layers in a station, and the

[2]In fact, an F module may be considered as two separate modules, since the straws terminate in the middle with the read-out electronics at the top and bottom of the module.

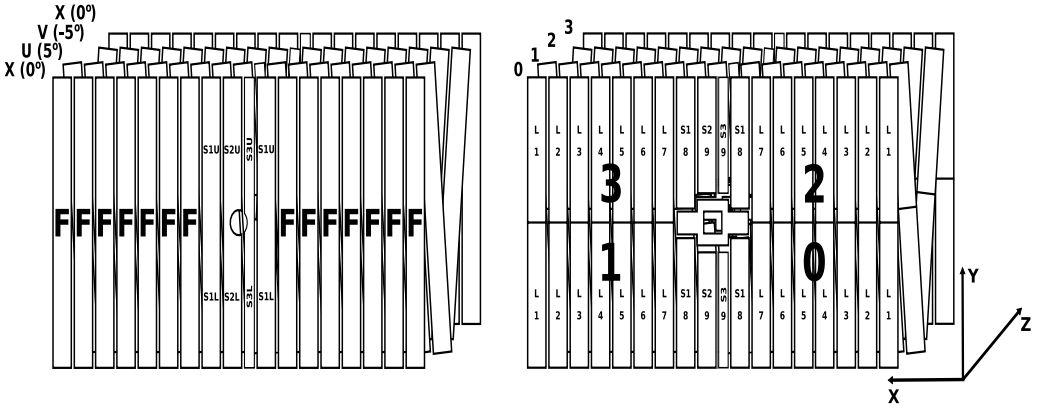

Fig. 2.3: (Left): Configuration of the layers inside an OT-station **(Right):** Numbering scheme for stations, layers, quarters and modules.

layout of the modules in a layer. Notice that the top S modules are coupled to the bottom S modules. Fig. 2.3(right) shows the detector description implementation and the numbering scheme used in the simulation (the stations are numbered 1, 2 and 3). Observe that the numbering scheme adopted here fully reproduces the hardware numbering scheme described in Ref [11]. Not shown in the Fig. 2.3 are the C-frames, which are also included in the description.

The modules are the basic building blocks of the Outer Tracker, i.e. each module is a stand-alone detector unit. A module consists of two staggered layers of straws sandwiched between two panels and side walls, see Fig. 2.4.

The widths of an F, S1 and S2 module, all containing 64 straws per mono-layer, is 340 mm and the width of an S3 module, which has 32 straws per mono-layer, is 172 mm. All modules are 32 mm thick. The lengths of the modules in the detector description are listed in Tab. 2.2. These, approximately, correspond to the lengths of the straws inside the LHCb acceptance. The lengths of the straws are such that they overlap with the IT making it possible to align the IT and OT with respect to each other. Notice that in the detector description, Fig. 2.3(right), the S modules are not coupled, instead the couplings are represented by a cross around the beam pipe.

Module	Length [mm]
F	4810
S1	2305
S2	2213
S3	2213

Tab. 2.2: OT Module lengths.

In the detector description the straws are represented by a single sensitive volume with the straw mate-

rials smeared over the volume[3]. The volume is determined by the number of straws in a module, the pitch in x, the pitch in z and the epoxy used to glue the straws to the panels, see Fig. 2.5.

Similarly, a panel/side wall, which is composed of multiple layers of different materials, is represented by single volume with the materials smeared over the volume, Fig. 2.5.

An S module coupling is composed of a piece of Rohacell sandwiched between two panels.

[3]One could add the straws for a more detailed description but at the cost of a slower simulation, i.e. more **CPU** time

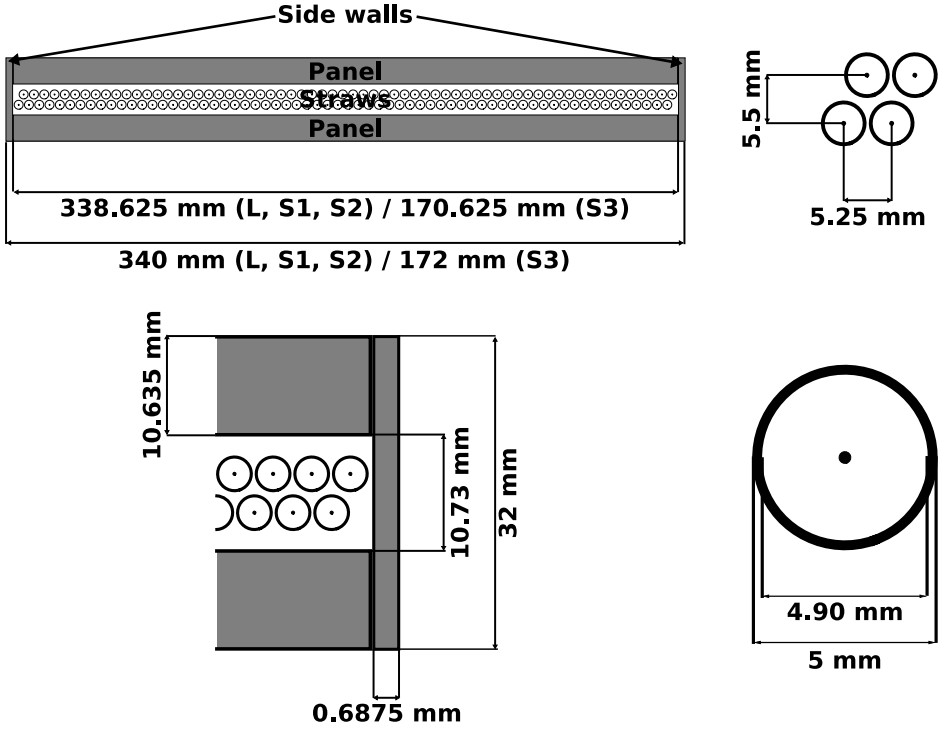

Fig. 2.4: Geometry, structure and dimensions of an OT Module.

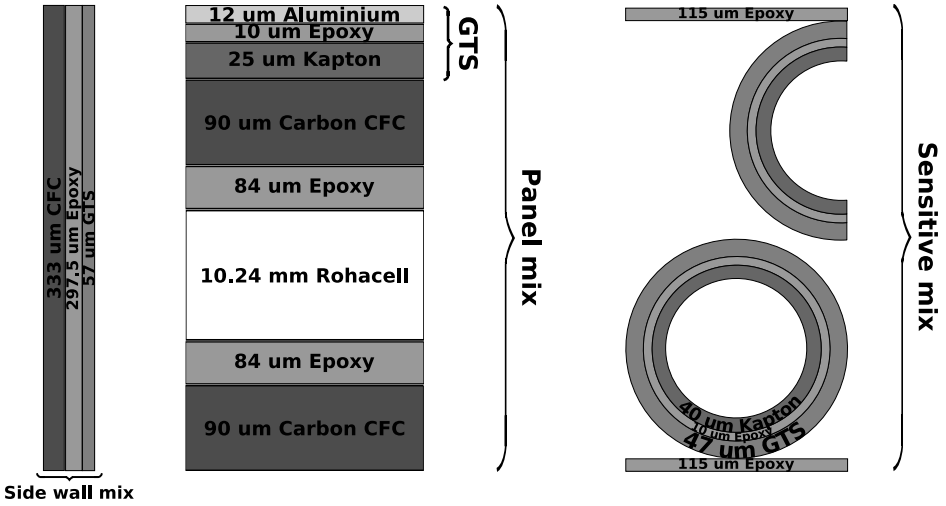

Fig. 2.5: OT Module materials.

Tab. 2.3 lists the composition and density of the OT materials used in the description description. Fig. 2.6 shows the radiation length X/X_0 as a function of η *vs* ϕ for OT station T3 as described in the simulation. The C-Frames at low η are clearly visible, as well as the S module couplings at high η. The average X/X_0 is 3.1%, while the X/X_0 for the region within the acceptance of the LHCb detector is 3.0%. Which is in good agreement with the $X/X_0 = 2.98\%$ determined in [12].

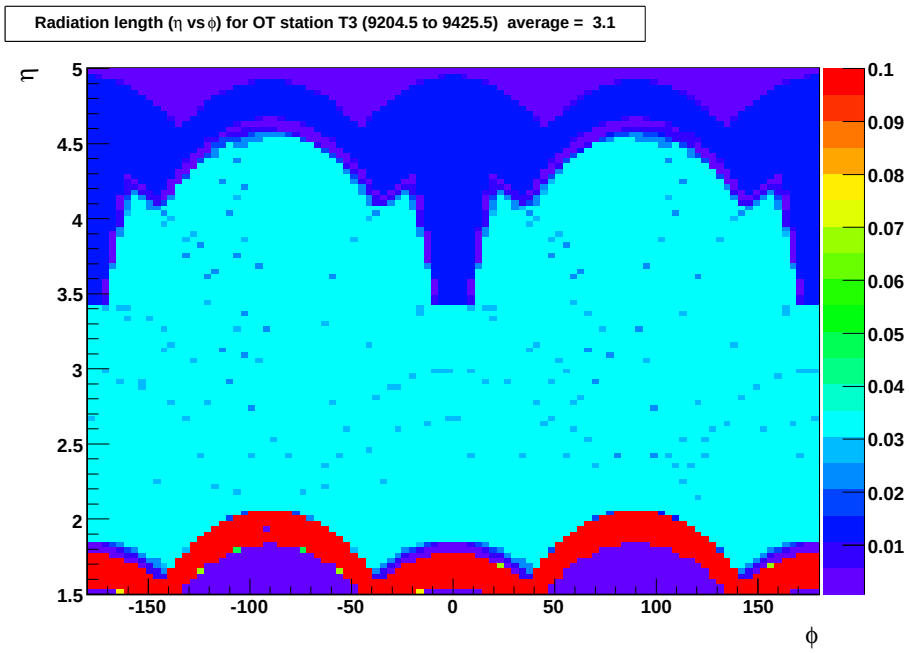

Fig. 2.6: Radiation length X/X_0 as a function of η *vs*ϕ for OT station T3.

Material	Density [g/ cm^3]	Epoxy	GTS	Kapton	CFC	Rohacell
Sensitive	0.1067	0.2634	0.4548	0.2818	-	-
Panel	0.0893	0.1765	0.0926	-	0.3465	0.3844
Side wall	0.1236	0.3686	0.0985	-	0.5328	0.3844

Tab. 2.3: Compositions of OT materials.

3 Simulation

The OT detector description covered in Sec. 2 is used in Gauss/Geant to simulate Monte Carlo Hits (**MCHit**s) in the OT which are then "digitised" in Boole, i.e. the hits are converted to TDC signals. This section covers the digitisation procedure starting from **MCHit**s to "real world" TDC signals. In the next section we will discuss the performance of the OT based on the simulation described here.

An **MCHit** is composed of an entry and exit point and in the case of the OT it is the entry and exit point in a sensitive layer, see Fig. 3.1. For a given entry and exit point one can easily determine the hit straws in the range given by the entry and exit points, since the sensitive layer is determined by the number of straws in a layer and their pitch in x and z.

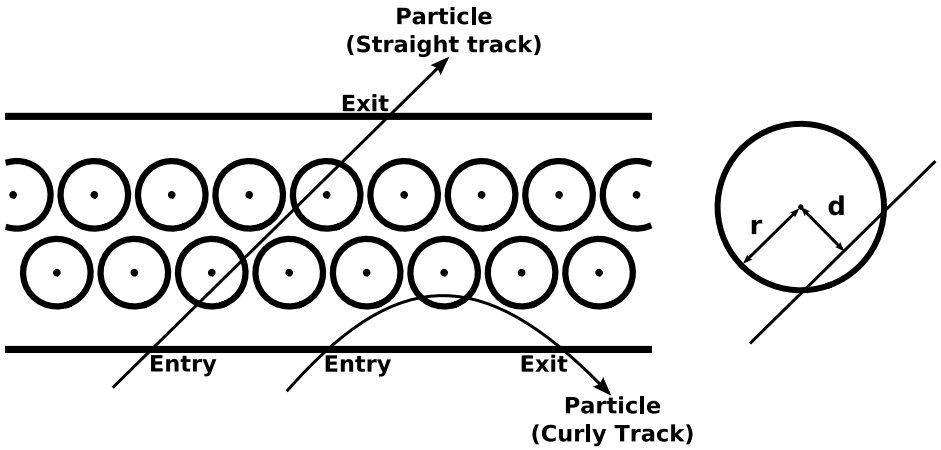

Fig. 3.1: MCHit in an OT module.

For each straw in the range given by the entry and exit points the "drift distance", d, is calculated and compared to the cell radius, r. If $d < r$ for a given straw then it, probably, was hit. The "drift distance" is simply the distance of closest approach (doca) between the wire and the track, which is a good approximation of the drift distance of the electrons that reach the wire first, i.e. the rising edge in the signal which is also the TDC time. Unfortunately, this only works well for straight tracks and not for curly tracks, i.e. low momentum particles.

For the F modules one also needs to check whether the hit is inside the efficient region (the region around $y = 0$) of a mono-layer, see Fig. 3.2.

Also, since the readout window of the OT is 75 ns and the bunch crossings occur every 25 ns one also needs to take spill-over hits in neighbouring bunch

crossings at -50 ns, -25 ns, 25 ns and 50 ns into account[4].

From these hit straws a "signal" deposit (**MCOTDeposit**) is created for each straw[5].

An **MCOTDeposit** is composed of an **MCHit**, a channel id (**OTChannelID**), the deposit time $t_{deposit} = t_{tof} + t_{spill}$ (where t_{tof} is the time-of-flight of the particle and $t_{spill} = \{-50\,\text{ns}, -25\,\text{ns}, 0\,\text{ns}, 25\,\text{ns}, 50\,\text{ns}\}$ is the spill time), an absolute drift distance and the left-right ambiguity of the hit.

The next step in the simulation, once all deposits have been created, is to simulate the idiosyncrasies of the OT: single cell efficiency, drift distance smearing, drift distance-to-time conversion (rt relation), cross talk, random (electrical) noise, deadtime and double pulse effect. This involves either deleting/modifying signal deposits or creating "noise" deposits.

The single cell efficiency is given by

$$\epsilon(l) = \eta_0(1 - e^{-\rho l}) \tag{3.1}$$

where $l = 2\sqrt{r^2 - d^2}$ is the path length through a straw, r is the inner radius and d is the drift distance, $\eta_0 = 0.99$ is the plateau efficiency, and $\rho = 3.333\,\text{mm}^{-1}$ (for a gas mixture of 70% Ar and 30% CO_2) is the average number of ionisations per unit length. The values of ρ and η_0 have been taken from measurements done at the 2005 Test Beam (see [13]). From Eq. 3.1 one can deduce, and as can be seen in Fig. 3.3, that the efficiency drops for tracks close to the straw wall, where $(1 - e^{-\rho l})$ gives the probability for having at least one efficient ionisation. The average integrated efficiency is 98.6%. In the simulation a signal deposit is deleted if the single cell efficiency of the corresponding straw is $\epsilon(l) = 0$.

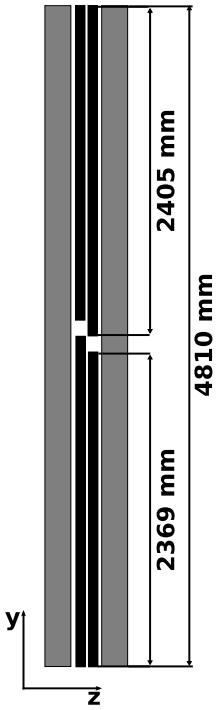

Fig. 3.2: F module.

The uncertainty on the drift distance is simulated by smearing the absolute drift distance, i.e. the distance of closest approach, of the signal deposit with a single Gaussian with a width of $\sigma = 200\,\mu$m, in space. This can lead

[4]These are known as **PrevPrev**, **Prev**, **Next** and **NextNext** in the simulation. Currently we do not simulate spill-over hits coming from **NextNext**. Instead we "copy" hits from the **PrevPrev** spill to the **NextNext** spill with a spill time of 50 ns. Which is statistically incorrect.

[5]Note that since a **MCHit** is "per layer" it is possible to have more than one **MCODeposit** per **MCHit**.

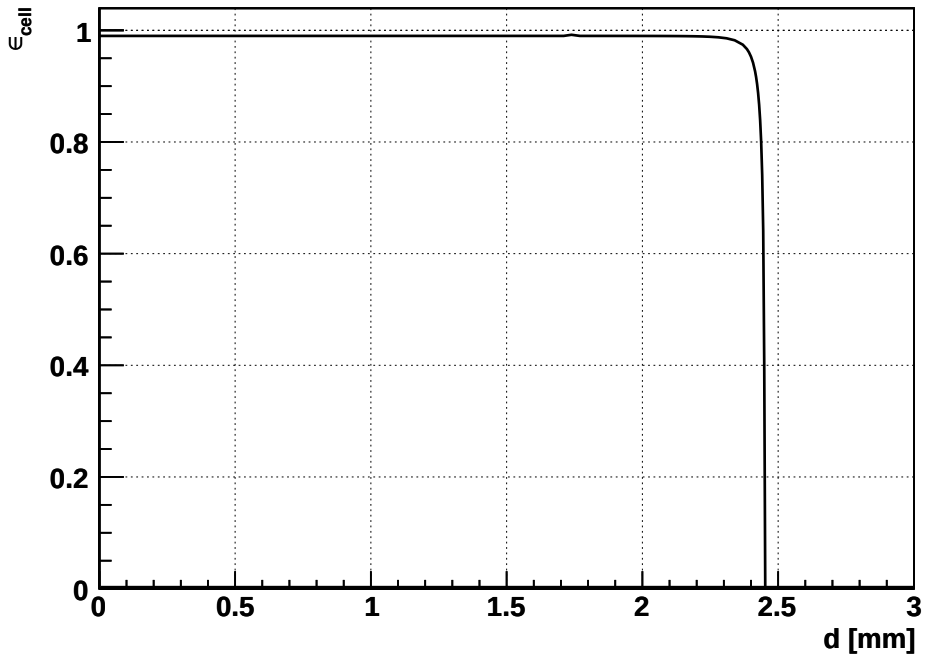

Fig. 3.3: Single cell efficiency, ϵ_{cell} as a function of the distance, d, to the wire. The average integrated efficiency, $d < r = 2.45\,\text{mm}$, is 98.6%.

to a negative smeared drift distance if a hit is close to the wire, in which case the ambiguity is flipped, or to a smeared drift distance greater than the cell radius, of up to 3 mm, if a hit is close to the cathode wall[6].

The rt-relation in the simulation is a linear relation that gives the drift distance as a function of the drift time

$$d(t) = v_{drift}t = rt/t_{max}, \tag{3.2}$$

where v_{drift} is the drift velocity and t_{max} is the maximum drift time. In the simulation the drift time is calculated for each signal deposit using Eq. 3.2 which, together with propagation time along the wire, gives a corrected deposit time

$$t_{deposit} = t_{tof} + t_{spill} + t_{drift} + t_{prop}. \tag{3.3}$$

Random (electrical) noise due to instabilities in a straw or from the readout electronics is about 10 kHz per channel. It is simulated by creating

[6]It has been proposed to smear the drift distance in time to correctly take effects close to the wire and cathode wall in to account.

deposits for each readout channel. A noise deposit contains only the channel id and the readout time of the channel. It does not contain a **MCHit**, since it does not originate from a hit.

Cross talk is the electrical pick-up of signals in neighbouring straws in a mono-layer. The fraction of cross-talk hits per channel in the simulation is 5%. It is simulated by copying a signal deposit in a channel to its neighbours. A cross talk deposit contains the channel id of the straw that picked up the signal and the hit information, minus the **MCHit**, of the original deposit.

The analog dead-time of the ASDBLR (**A**mplifier-**S**haper-**D**iscriminator with **B**ase**L**ine **R**estoration), i.e. the total time it takes to process a hit, is 17 ns, depending on the pulse height of the hit. The output of the ASDBLR is then passed on to the OTIS (**O**uter Tracker **T**ime **I**information **S**ystem) which is a TDC (**T**ime to **D**igit **C**onverter). It takes the signal from the ASDBLR and returns a 6 bit TDC time plus 2 bits for the bunch crossing, i.e. spill, from which the hit originates. The dead-time for the the TDC conversion is around 25 ns, thus greater than the dead-time of the ASDBLR. Therefore the analog dead-time in the simulation was chosen to be 25 ns. The readout window of the OTIS is 75 ns and can be readout in single-hit mode or multiple-hit mode. In the former case, what is aslo done in the simulation, only the first hit found inside the 75 ns readout window is read out. This gives an effective "dead-time" of 75 ns. In multiple hit mode all found hits from all 3 bunch crossings are read out. For more details on the ASDBLR and OTIS see [14].

$$t_{pulse} = t_{deposit} + 30\,\text{ns}\,. \tag{3.4}$$

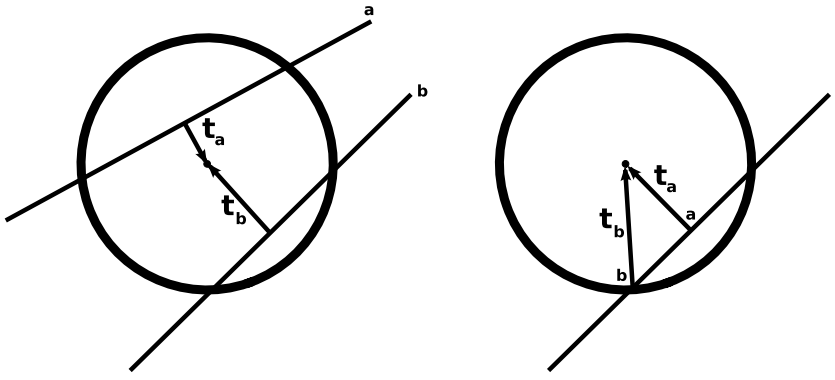

Fig. 3.4: Double Hit and Double Pulse.

It is possible to record more than one TDC time for a hit, e.g. if the delay $(t_b - t_a)$ between drift electrons coming from a and from b is greater than the

analog dead-time, see Fig. 3.4. This is known as the double pulse effect. From an electronics point of view, the double pulse effect is the same as a double hit, i.e. two tracks in a straw, since there is no way of distinguishing between a double pulse effect or a double hit. In the simulation the probability for a hit to give a double pulse is 30%. It is simulated by creating deposits for each signal deposit and contains the channel id of the signal deposit and the time of the signal deposit plus the time of the second pulse (= 30 ns).

The next and final step in the simulation is to sort the **MCOTDeposit**s by channel and time and create the associated TDC times (**MCOTTime**) which are then encoded and put in the raw buffer according to the format described in [15]. At this stage the analog dead-time, 25 ns, and the readout window, 75 ns, is also applied, i.e. a new **MCOTTime** is only created if the TDC time of the current **MCOTDeposit** is outside the dead-time of the previous **MCOTDeposit** and is outside the readout window in single-hit mode.

4 Performance

This section gives an overview of the OT performance. The numbers quoted and plots were obtained with Boole v14r2. The data sample used was 2000 $B_d^0 \to J/\psi(\mu\mu)K_S$ un-triggered events generated at a luminosity of $2 \times 10^{32}\,\mathrm{cm}^{-2}\mathrm{s}^{-1}$, unless otherwise indicated.

4.1 Hit profile for OT station T3

Fig. 4.1 shows the hit profile for T3 for 200 events 2000 $B_d^0 \to J/\psi(\mu\mu)K_S$. Note the particle flux is higher around the IT, i.e. the region around the cross. The same can be observed when looking at occupancy vs x.

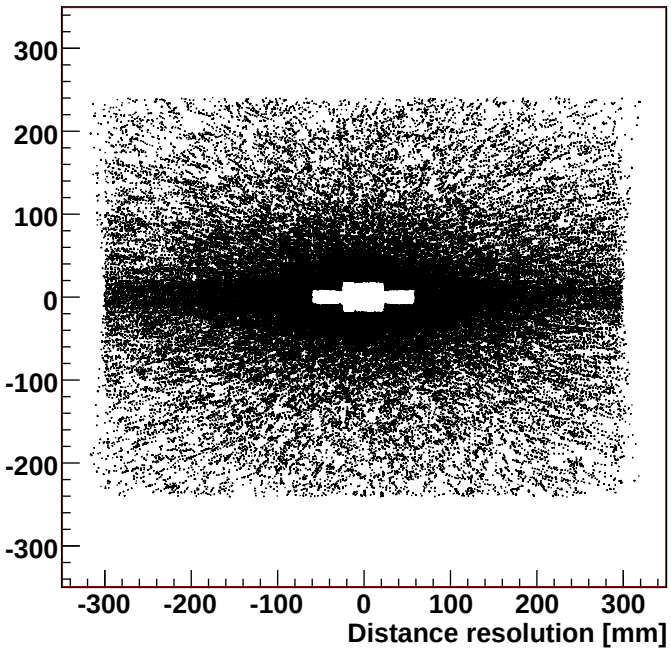

Fig. 4.1: Hit profile for OT station T3.

4.2 MCOTDeposit spectrum and OTTime spectrum for OT station T3

Since the readout window of the OT (= 75 ns) is a factor 3 larger than the accelerator bunch crossing time of 25 ns, events from previous or next bunches have to be considered.

Fig. 4.2 figure shows the **MCOTDeposit** spectrum sorted according to the spills from which the **MCHit**s, that make up the **MCOTDeposit**s, originate. The **MCOTDeposit**s in the current spill are from $B_d^0 \to J/\psi(\mu\mu)K_S$ events. The **MCOTDeposit**s in the previous and next spills are from minimum-bias events. Notice that the fraction of **OTMCDeposit**s from **Prev** and **Next** spills inside the readout window of 75 ns is greater than that from **PrevPrev** and **NextNext**. A detailed study on the effect on the occupancy of the various spills can be found in [16].

Fig. 4.3 shows the **OTTime** spectrum for OT station T3 after the creation and encoding of **MCOTTime**s, and the decoding of the raw buffer. An **OTTime** contains a **OTChannelID** and a calibrated TDC time. The calibrated TDC time is the TDC time stored in the **OTChannelID** converted to ns and corrected with a t_0 offset. Notice that the shape of the **OTTime** spectrum resembles that of the **MCOTDeposit**s that fall within the 75 ns readout window. Also, a t_0 correction has been applied, hence the spectrum starts at 0 ns.

Tab. A.5 shows the various average contributions to the **OTTime**s. The 68.7% are signal events of which 43.5% are from primary interactions and 25.1% are from secondary interactions. A small percentage is "un-classifiable". 1.4% is noise and 5% is cross-talk which corresponds to the values used in the simulation. 24.9% is spill-over of which a greatest fraction is from the **Prev** and **Spills**.

Fig. 4.4 shows from where the **MChits** originate in the LHCb detector that contribute to **OTTimes**. **MCHits** originating from the VeLo, TT and RICH1 ($z < 300$ cm) are clearly distinguishable. As well are hits from the Magnet and beam pipe supports (400 cm $< z <$ 700 cm), and hits from the IT, OT and RICH2 ($z > 700$ cm).

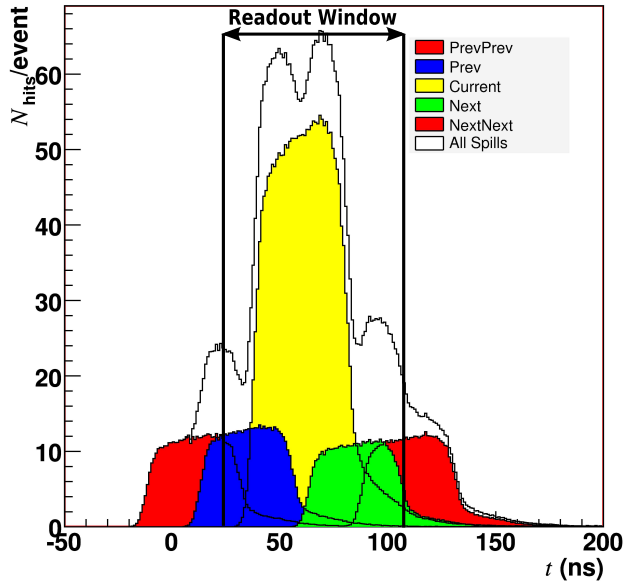

Fig. 4.2: MCOTDeposit spectrum for OT station T3.

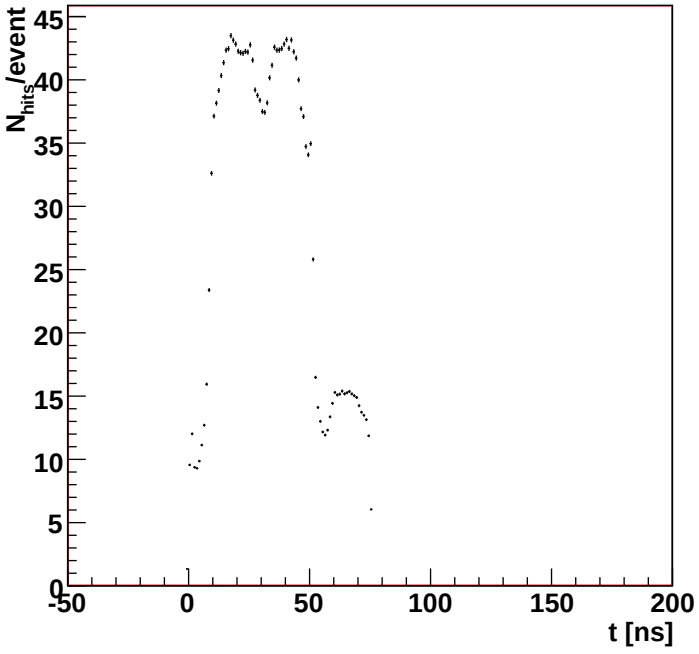

Fig. 4.3: OTTime spectrum for OT station T3.

OTTime Contributions	Amount in %
Physics Events	
Primary	43.4
Secondary	25.1
Unknown	0.2
Subtotal	68.7
Noise	1.4
Cross-talk	5
Spill-over events	
PrevPrev + NextNext	5.8
Prev	10.4
Next	8.7
Subtotal spill over events	24.9

Tab. 4.1: Various contributions to the OTTimes.

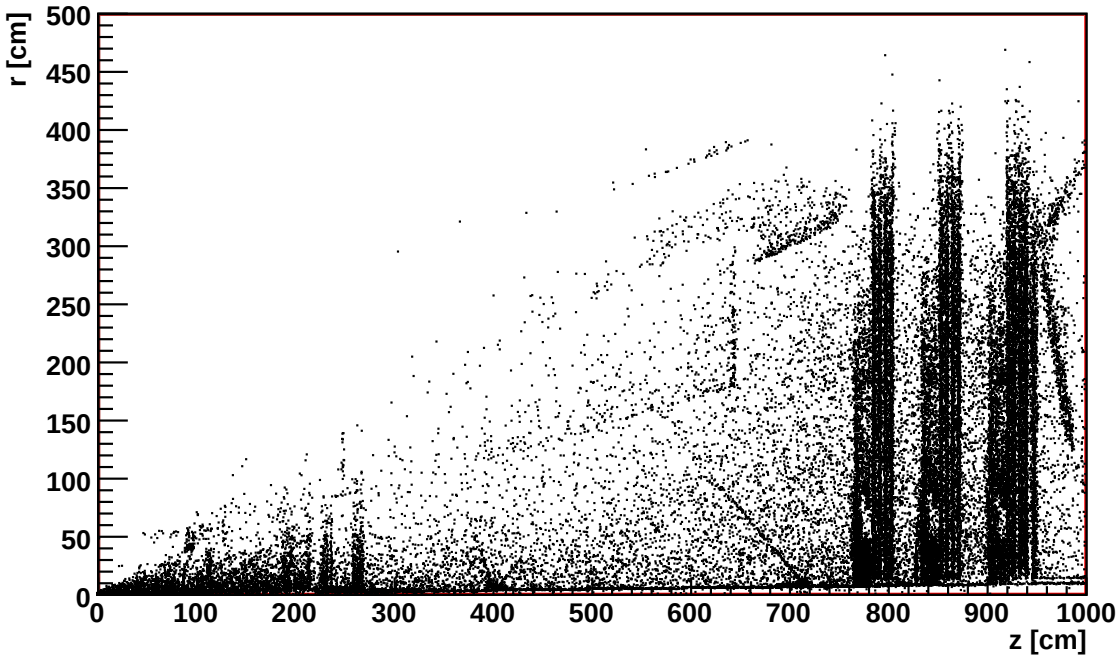

Fig. 4.4: *r vs z* **MCHit** distribution of **MCHit**s that contribute to **OTTime**s.

4.3 Occupancy

Fig. 4.5 shows the occupancy vs x for OT station T3. Notice that in the region close to the IT, where the particle flux is the high, the occupancy is 11%. The average occupancy is 6%. The occupancies are higher compared to [16] due to a more realistic description of the beam pipe, IT [17], and OT, which results in higher material budget compared to DC04 [18, 19].

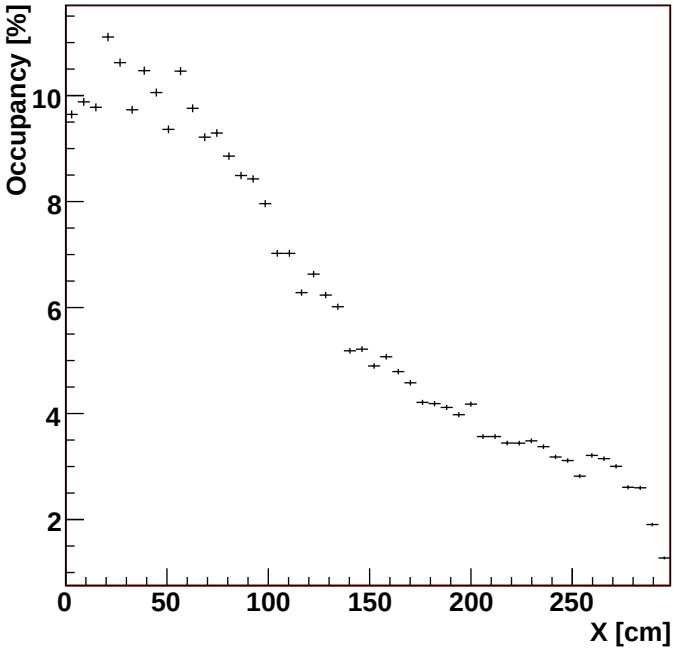

Fig. 4.5: Occupancy vs x for OT station T3.

4.4 Drift distance resolution

Fig. 4.6 shows the drift distance resolution, obtained by converting the drift time to a distance via the rt-relation and comparing it to the MC drift distance. The resolution obtained, by fitting the distribution to a single Gaussian, is 230 μm. Fitting the distribution to a double Gaussian, Fig. 4.7, yields a core resolution of 208 μm at 97%. The second Gaussian has a resolution of 1.125 mm. The resolution of 208 μm is in agreement with the value used in MC and with the value obtained in the 2005 test beam [13].

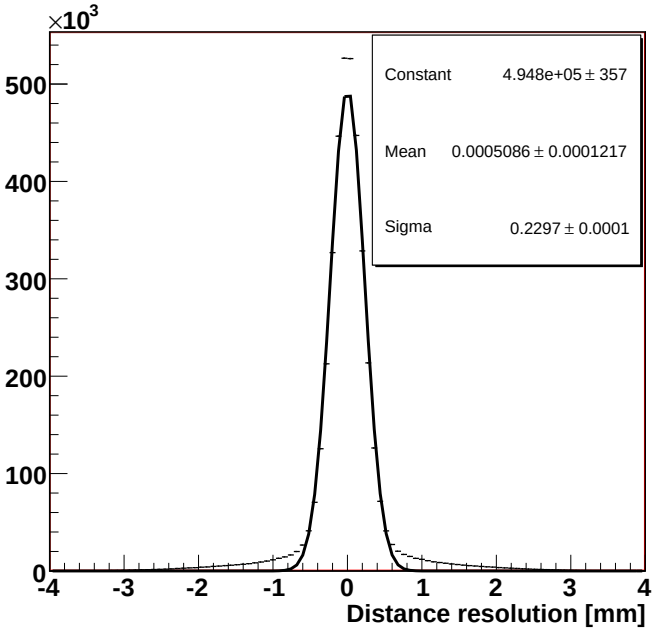

Fig. 4.6: Drift distance resolution fitted to a single resulting Gaussian with $\sigma = 230\,\mu$m.

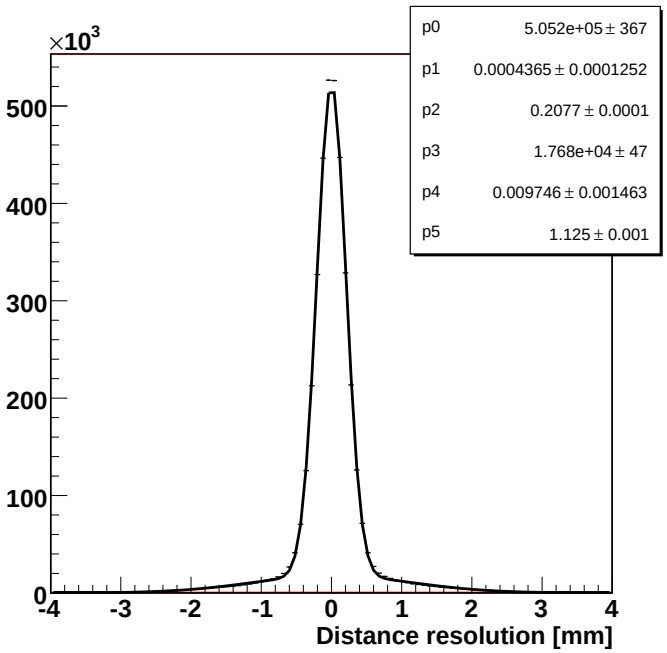

Fig. 4.7: Drift distance resolution fitted to a double Gaussian with a core resolution of $208\,\mu$m at 97%.

4.5 Efficiency

The average hit efficiency, defined as the number of **MCHit**s associated to at least one **OTTime** divided by the total number of **MCHit**, is 96.1%. The average hit efficiency is composed of three parts, since a **MCHit** can lead to 1 or more **MCOTDeposit**s per layer. The first part is the hit efficiency for a single hit in a layer and is 14.2%. The second part is the hit efficiency for a double hit in a layer and is 68.2%. The last part is the hit efficiency for a three or more hits in a layer and is 13.7% When one applies a momentum cut of 2 GeV the efficiency increases from 96.07% to 98.8%.

The average monolayer hit efficiency is 87.6% this yields a average cell efficiency, taking the inefficient regions a layer into account, of

$$e_{cell} = 5.25/4.90 * 87.6\% = 93.9\%. \tag{4.1}$$

For a momentum cut of 2 GeV the average monolayer efficiency is 92% and the the average cell efficiency is 96%.

A Default options used in Boole

This appendix lists the default options used for the digitisation of the OT in Boole.

Option	Type	Description	Default Value
spillVector	**vector<string>**	Vector of spills	**{"/PrevPrev/", "/Prev/", "/", "/Next/", "/NextNext/"}**
spillTimes	**vector<double>**	Time offset of spills in ns	**{ −50, −25, 0, 25, 50}**
addCrossTalk	**bool**	Add cross-talk?	**true**
crossTalkLevel	**double**	Level of cross-talk	**0.025**
addNoise	**bool**	Add noise?	**true**
addPulse	**bool**	Add double pulses?	**true**
PulseTime	**double**	Time offset of double pulse in ns	**30**
PulseProbability	**double**	Probability for a double pulse	**0.3**
noiseToolName	**string**	Name of noise tool	**"OTRandomDepositCreator"**

Tab. A.1: Default options for the algorithm MCOTDepositCreator.

Option	Type	Description	Default Value
etaZero	**double**	Plateau efficiency	**0.99**
rho	**double**	Average number of ionisations per unit length in mm^{-1}	**3.333**

Tab. A.2: Default options for the tool OTEffCalculator.

Option	Type	Description	Default Value
NoiseRate	**double**	Noise rate in kHz	**10.0**
ReadOutWindowToolName	**string**	Name of read out tool	**"OTReadOutWindow"**

Tab. A.3: Default options for the tool OTRandomDepositCreator.

Option	Type	Description	Default Value
startReadoutGate	**vector<double>**	Start of read out gates in ns	**{28, 30, 32}**
sizeOfReadoutGate	**double**	Size of gate in ns	**75**

Tab. A.4: Default options for the tool OTReadOutWindow.

Option	Type	Description	Default Value
DeadTime	**double**	Analog dead-time in ns	**25**
countsPerBx	**int**	Counts per bunch crossing	**64**
numberOfBx	**int**	Number of bunch crossings	**3**
timePerBx	**double**	Time per bunch crossing in ns	**25.0**
singleHitMode	**bool**	Single hit mode?	**true**

Tab. A.5: Default options for the algorithm MCOTTimeCreator.

References

[1] The LHCb Collaboration, P.R. Barbosa *et al.*, *Outer Tracker Technical Design Report*, CERN/LHCC 2001-024, Sep. 2001.

[2] The LHCb Collaboration, P.R. Barbosa *et al.*, *Inner Tracker Technical Design Report*, CERN/LHCC 2002-029, Nov. 2002.

[3] M. Needham, *Performance of the LHCb Track Reconstruction Software*, LHCb 2007-144, Dec. 2007

[4] M. Merk *et al.*, *An improved digitization procedure for the outer tracker*, LHCb 2001-055, Mar. 2003.

[5] M. Merk *et al.*, *Optimizing the Outer Tracker near the y=0 region*, LHCb 2003-019, Mar. 2003.

[6] J. v. Tilburg, *Outer Tracker Software*, LHCb 2003-062, Jul. 2003.

[7] J. Nardulli and J. v. Tilburg, *Outer Tracker Event Data Model*, LHCb 2005-004, Jan. 2005.

[8] The LHCb Collaboration, S.Amato *et al.*,*LHCb Techical Proposal*, CERN/LHCC 1998-04, Feb. 1998

[9] The LHCb Collaboration, R. Nobrega *et al.*, *LHCb Reoptimized Detector Design and Performance Technical Design Report*, CERN/LHCC 2003-030, Sep. 2003.

[10] S. Bachmann and A. Pellegrino, *Geometry of the LHCb Outer Tracker (Part I)*, LHCb 2003-035, May 2003.

[11] A.Pellegrino *et al. Address Scheme for the Outer Tracker FE Electronics*, LHCb 2003-041, Sep. 2003.

[12] J. Nardulli and N. Tuning, *A Study of the Material in an Outer Tracker Module*, LHCb 2004-114, Dec 2004.

[13] G. Van Apeldorn *et al.*, *Beam Test of the Final Modules and electronics of the LHCb Outer Tracker in 2005*, LHCb 2005-076, Oct. 2005.

[14] L.B.A. Hommels, *The Tracker in the Trigger of LHCb*, CERN-THESIS/2006-058, Oct. 2006.

[15] J. Nardulli *et al.*, *Outer Tracker DAQ Data Format*, LHCb 2004-033, Jan. 2005.

[16] J. Nardulli *et al.*, *Outer Tracker Occupancy Studies*, LHCb 2005-092, Dec. 2005.

[17] K. Vervink and A. Perrin, *The Inner Tracker detector description and its implementation in the XML database*, LHCb 2006-018, May 2006.

[18] M. Needham and T. Ruf, *Estimation of the material budget of the LHCb detector*, LHCb 2007-025, Mar. 2007.

[19] M. Needham, *Silicon Tracker Occupancies and Clustering* , LHCb 2007-025, Apr. 2007.